Odor specificity and response reliability of mushroom body-extrinsic neurons in the honeybee

Martin Fritz Strube-Bloss, Farzad Farkhooi, Martin Paul Nawrot and Randolf Menzel

Abstract

The insect mushroom body [MB] integrates sensory information from different modalities with reward-related signals and is known to be directly involved in memory formation. However, little is currently known about stimulus representation at the single-cell level in the MB. Here we investigated odor representation and response reliability in a population of extrinsic neurons [ENs] in the honeybee that form the output of the MB. We performed extracellular long-term recordings of single ENs while the subjects were exposed to repeated stimulations with 10 different odors. We found that ENs are generally odor-unspecific, showing responses to many different odors. Odor tuning of the trial-averaged response firing rate was weak in most of the cells. Trial-by-trial analysis revealed that most cells responded unreliably, i.e. they responded in some of the trials but not in others. Our results indicate that the neural population activity at the MB output level does not reliably represent sensory stimuli.

Introduction

Understanding the representation of sensory information at the level of different neuropils is the prerequisite for investigating modulatory processes across a sensory pathway. In insects the olfactory sensory neurons [ORNs] converge into the antennal lobe [AL], whose glomerular structure is homologue to that of vertebrates. In the honeybee the AL projection neurons [PNs] send their branches to higher brain areas via different axonal tracts (Mobbs, 1982; Bicker et al., 1993). The lateral antenno-cerebral tract [l-ACT] and the medial antenno-cerebral tract [m-ACT] are two of these which are composed of uniglomerular PNs and target the lateral horn and the mushroom body

[MB] input region, the calyx, which consist of Kenyon cells [KC] (Abel et al., 2001; Müller et al., 2002).

The AL of the honey bee consists of 160 glomeruli (Flanagan and Mercer, 1989; Galizia et al., 1999a). Optical imaging studies show that at these levels odors are specifically represented in complex spatio-temporal activity patterns of excited and inhibited glomeruli (Sachse and Galizia, 2002). At first glance the investigation of learning-induced changes at the PN level led to contradictory results. Peele et al. (2006), for example, found that uniglomerular AL projection neurons in honey bees show no significant difference in odor-evoked activity after classical odor conditioning. Faber et al. (1999) found learning-induced changes and an increase in activity as response to the rewarded, but not to the unrewarded odor after differential conditioning in the AL.

At the next higher level, the MB, which consists mainly of KC (Heisenberg, 2003), olfactory information is spread into a multi-dimensional space of KC activity (about 200,000 in cockroaches, 170,000 in honey bees, 50,000 in locusts and 2,500 in *Drosophila*). KCs are believed to also respond highly odor-selectively and sparsely in *Drosophila* (Turner et al., 2007) as well as in locusts (Stopfer et al., 2003; Jortner et al., 2007). There is much evidence that the MBs are higher-order centers of the insect brain where olfactory, visual and mechano-sensory information is integrated. The MBs are involved in the regulation of motor actions like walking behavior (Martin and Heisenberg, 1998), and they were described long ago as a center for learning and memory formation (Dujardin, 1850; Strausfeld, 1998, review). Amnesic treatments support the theory that the network formed by the MB is directly involved in memory consolidation. In honey bees, the conditioned response probability was greatly reduced when the MBs had been treated shortly after a single learning trial (Erber et al., 1980; Menzel et al., 1974). In *Drosophila* the different MB-branches (γ-lobe, α/β-lobe) are involved differentially in memory formation (Zars et al., 2000; Pascual and Preat, 2001). Imaging KC activity, for example, showed that a branch-specific memory trace is formed between 3 to 9 hours after conditioning only in the alpha-branch of the MB (Yu et al. 2006).

In the honey bee around 400 extrinsic neurons [ENs] read out the activity pattern of the KCs and form the output of the MB (Rybak and Menzel, 1993). The pedunculus-extrinsic neuron one [PE1] is one of the best-studied identified cells extrinsic to the

alpha lobe, with large branches collecting its information from the KCs. It changes its response during classical odor conditioning (Mauelshagen, 1993). Electrical stimulation of the KC leads to formation of associative long-term potentiation (LTP) in the PE1 (Menzel and Manz, 2005). Extracellular long-term recordings also document that PE1 shows a reduction in response to the rewarded stimulus after the subject has associated an odor with a reward (Okada et al, 2007). Furthermore, experiments in different insect species have shown that ENs are definitly involved in learning-induced plasticity changes, for example, in locusts where spike time-dependent plasticity [STDP] occurs between KCs and β-lobe neurons (Cassenaer and Laurent, 2007), or in *Drosophila* where a delayed memory trace is formed after 30 min only in the vertical (α-lobe) branch of the dorsal-paired medial neuron [DPM] which is an odor generalist (Yu et al. 2005). However, not much is known about the general representation of olfactory stimuli at this neuronal level.

In the present study we focus on other - so far unidentified - ENs by applying extracellular recordings from the ventral part of the alpha-lobe of the MB. ENs that can be recorded at this part of the alpha-lobe can be related to the A1, A2, A4, A5 and A7 clusters. The projection fields of most mentioned EN types are restricted to only one protocerebral hemisphere where they connect the MB with the neuropils around the alpha lobe and with the lateral protocerebral lobe [LPL]: only the A7type connects the ipsilateral brain side with the contralateral MB (Rybak and Menzel, 1993). In insects extracellular long-term recordings are successfully used to characterize the activity of single [MB] neurons in freely-moving cockroaches (Mizunami et al., 1993; Mizunami et al., 1998; Okada et al., 1999). In honey bees extracellular long-term recording were established to record the activity of the PE1 in a behaving animal during a classical conditioning experiment (Okada et al., 2007).

Here we adapted and modified these extracellular recording technique to increase the possibility of recording simultaneously from more than one unit, in an effort to lay the foundation for further studies which will focus on correlations between single neurons. We demonstrate that the general representation of odor stimuli, as compared to the input level of the MB, is rather unsparse. EN responses are odor-unspecific and rather unreliable regarding their reliability in responding to the same odor stimulus. Thus we

conclude that the neural population activity at the MB output level does not reliably represent sensory stimuli.

Material and Methods

Subjects

Forager honeybees were caught at the hive entrance in the afternoon, one day before the experiment. They were anesthetized on ice, and harnessed in metal tubes such that they could freely move their probosces and antennae. Bees were fed to satiation with 30% sucrose solution and kept at room temperature (26°C) overnight.

Odor stimulation and experimental paradigm

Odor-supplying device

A 12-channel-olfactometer was adapted from Galizia et al. (1997) and equipped with 5ml syringes (odor chambers). A constant air stream (1.5 m/s) was delivered from a Teflon tube (6 mm in diameter). The needles of the syringes were inserted into this Teflon tube. Odors were diluted in paraffin oil at a 10^{-2} concentration. Filter papers ($3cm^2$) were soaked in 10 µl of odor solution or pure paraffin oil as a control and placed in the syringes. During odor stimulation, which lasted 3 seconds, only 2.5 ml of the air volume of the 5 ml chambers were injected into the constant air stream to avoid concentration gradients. The Teflon tube's outlet was placed 1 cm away from the bee's head. An exhaust hood (tube with 10 cm diameter) was placed behind the bee to remove the remains of the presented odors. A Visual Basic Script (VBA 6.0, Microsoft, USA) written by Frank Schaupp was used to control the 12 fast magnetic valves (Lee, Westbrook, Connecticut) of the odor-supplying device. Time stamps of valve opening and closing were noted with the data acquisition system.

Experimental procedure

To investigate response reliability and odor specificity we repeatedly presented 10 different odors (2-octanol, octanal, 2-nonanone, 1-nonanol, cineole, linalool, limonene, eugenol, 1-heptanal, hexanal [Sigma-Aldrich Chemie GmbH], diluted by a factor of 100 in paraffin oil) and a control solution (pure paraffin oil) for 10 repetitions. Each time the odor was presented for 3 seconds during which the odor was injected into the constant air stream. Spontaneous activity of alpha-lobe-extrinsic neurons (ENs) was recorded for 3 min before starting the stimulation protocol from a total of 51 units in 23 animals. We tested the odor responses in 11 of these 23 animals (N=27 units).

Electrophysiology

Differential recording

A small unilateral window (1.5 x1.5 mm) was cut between the compound eye and the midline of the bee antennae. Head glands and trachea sacks above the alpha-lobe were removed, and the electrode was positioned at a depth between 100 and 250 µm. Following insertion, the whole gap was filled with two-component silicon (KWIK-SIL Sarasota, FL, USA) to prevent the brain from drying out and to fasten the electrode to the brain. Recordings could last for up to 30 hours. We usually terminated the recording after our experimental protocols were successfully completed.

Our electrodes consisted of three wires (polyurethane-coated copper wire, 14 µm in diameter [Electrisola, Escholzmatt, Switzerland]). Preparation of the electrodes was adopted from Ryuichi Okada (Mizunami et al., 1998; Okada et al., 1999) and modified to obtain three recording channels: Three wires were glued together with wax onto a tungsten wire (1-2 cm long and 100 µm in diameter) that was attached to a glass capillary. The glass capillary was fixed onto a custom-built adapter to allow a connection with the headstage amplifier (Headstage-27 Amplifier Neuralynx, Tucson, AZ, USA). Signals used for spike detection were measured differentially from all three electrode pair combinations using the Patch Panel (ERP-27, Neuralynx, Tucson, AZ, USA [see Fig.1]). The advantage of the differential wire combinations is illustrated in Figure 1. Channels 11, 12 and 13 represent the possible differential recording

combinations for the three wires. Channel 11 is the difference of channel 14 and 15, channel 12 of 16 and 14, and channel 13 is the differential combination of 15 and 16. The three separate channels (14, 15 and 16) are measured against the reference electrode, which is located inside the compound eye. The recording trace in the middle shows the activity of the M17 muscle, which innervates the bee's proboscis. Recording this channel is a direct access which simultaneously monitors the neuronal activity of single units into the brain and the animal's behavior. Note that voltages in this channel lead to strong activity in the single traces of the wires measured only against the reference electrode (14, 15 and 16) which could cause misinterpretation, whereas the differential channels are not influenced by the motor activity in M17 (channel 17). These traces (11, 12 and 13) reflect the local activity close to the tip of the electrode.

Using these raw signals we were able to identify and record from up to 5 units simultaneously. A silver 25 µm-diameter wire (Nilaco, Tokyo, Japan) inserted into the right compound eye served as the reference electrode. The electric signals were amplified by a Lynx-8 Amplifier (Neuralynx, Tucson, AZ, USA) with a 1-9000 Hz band-pass filter and digitized at a sampling frequency of 20 kHz. After importing the files into the Spike2 (Cambridge Electronic Design, Cambridge, UK) data format, we applied a software high-pass filter (>300 Hz) and semi-automatic spike sorting techniques (template-matching, see Fig. 2). A second silver 25 µm-diameter wire (Nilaco, Tokyo, Japan) was inserted between the right occellus and the compound eye to electrophysiologically monitor the proboscis extension response (PER), which is mediated by the M17 muscle (Rehder, 1987; see Fig. 1).

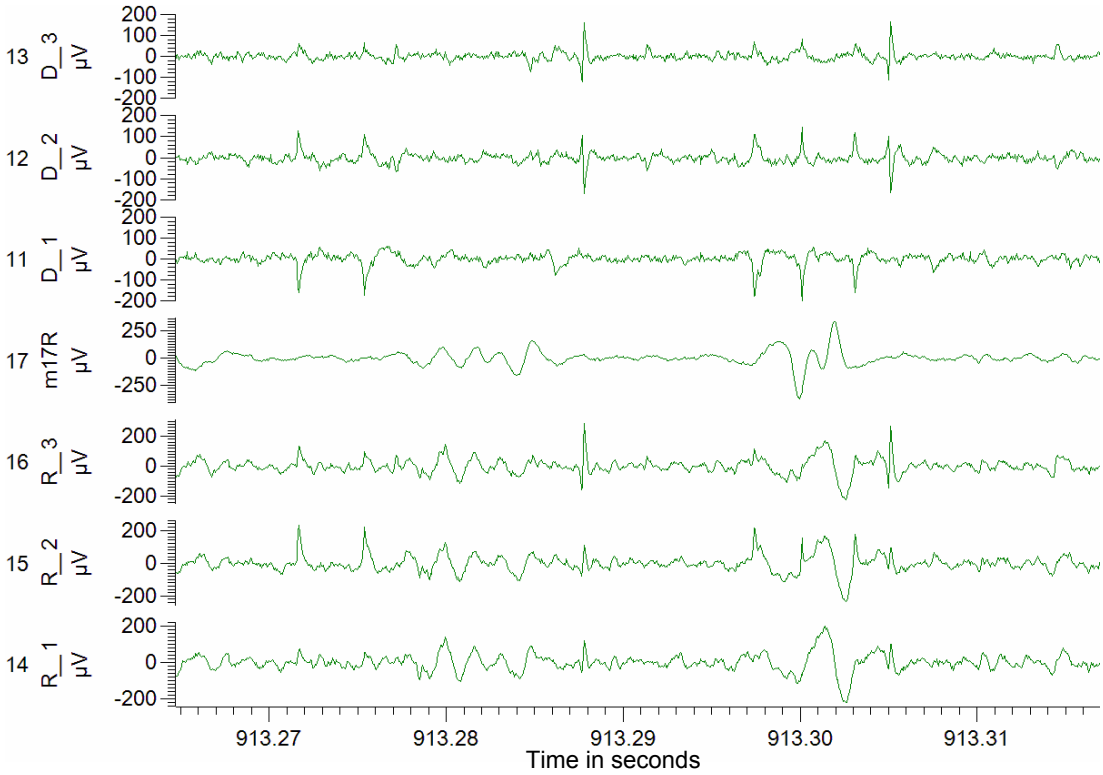

Figure1. Local neuronal activity is recorded via differential channel combinations. *The three single wires of the recording electrode are measured against the reference (lower 3 channels; 14, 15, 16). The activity of the M17 muscle as shown in the middle channel (17) has common influence on all three electrode signals. This common influence of the M17 is largely diminished in the 3 differential recording combinations (upper channels 11, 12, 13). All channels were filtered between 300 and 9000 Hz. Note that the differential recording combinations of the three wires were not affected by the M17 activity (17).*

Spike sorting

Individual neurons generate action potentials with a characteristic shape due to their intrinsic electrochemical dynamics. In addition, the extracellularly-recorded amplitude of a neuron spike depends on the position of that neuron relative to the electrode tip. Therefore differences in spike shape and amplitude can be exploited to classify action potentials of different neurons. For analyzing the activity of single alpha-lobe-extrinsic neurons only the differentially-recorded channels were used (Fig. 1). A template sorting with *spike 2* was performed on each channel. To assess the quality of the classification of spike events, a principal component analysis (PCA) was performed after sorting (Fig. 2B).

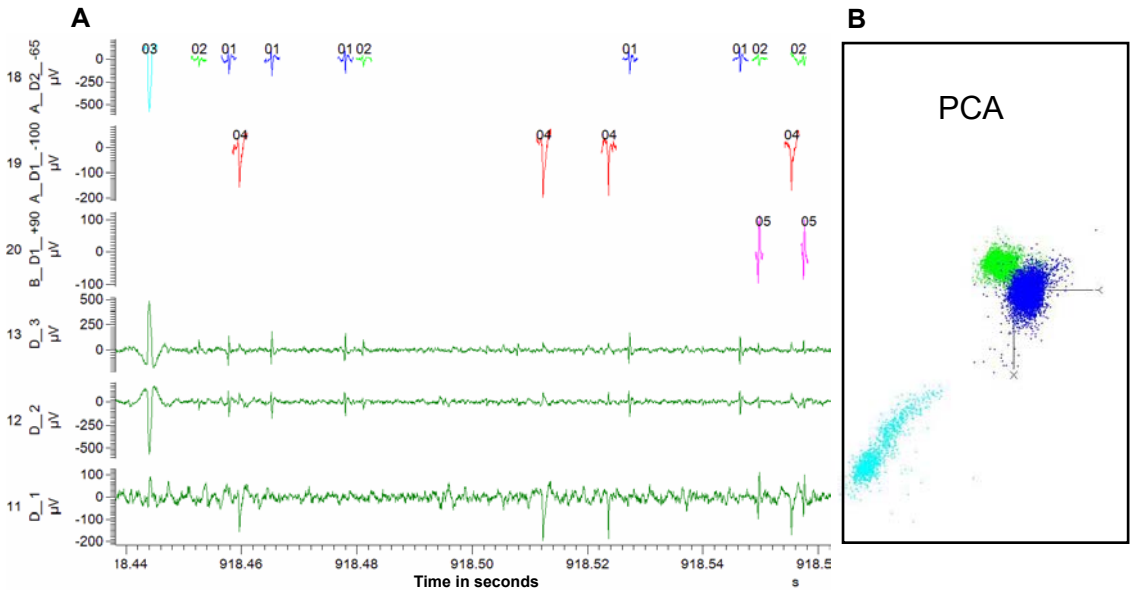

Figure 2. Extraction of 5 units by semiautomatic template sorting (Spike2). ***A*** *Single spike events were detected from the three simultaneously-recorded and filtered differential channels (11, 12, 13). Channel 20 comprised the events of unit 05 (magenta) detected from recording trace D_1 (chan. 11) with a threshold of +90 µV. On channel 19 the spikes of unit 04 (red) were detected from the differential recording trace D_1 (11) with a threshold of -100 µV. Channel 18 shows three different units (01/blue, 02/green, 03/turquoise) that were sorted from the differential recording trace D_2 (12) with a threshold of -65 µV.* ***B*** *Principal Component Analysis (PCA) of the three different event types (units) of channel 18 (01/blue, 02/green, 03/turquoise). Note that the clusters are well separated by their first three principal components.*

Data Analysis

Analysis of spontaneous activity

In a first step of our analysis we identified the longest stretch of stationary activity in each spontaneuse spike train. To this end, we measured the spike count in successive time bins of a fixed length of either 1 s or 500 ms, for lower (< 10 /s) or higher firing rate, respectively, and divided the total series of counts into equal groups of 30 bins. Each subseries of the counting process was then tested for stationarity, as described previously by Farkhooi et al. (submitted). We collected all ISIs from the longest stationary spike train of each neuron and estimated their distribution.

Response Detection and Reliability

To decide for each single stimulation if the presentation of an odor lead to a response in the recorded unit, we focused on the changes in the Inter-Spike-Interval (ISI) distribution. To this end we compared the ISIs in two observation windows (Fig. 3). One was the 3-second recording window before every stimulus onset. The second comprised the first 500 ms after the odor onset, when we observed the strongest change in the ISI distribution, as our observations suggested (see Fig. 6 and Fig. 11). We then pooled intervals in the spontaneous observation window from all trials. To detect a significant ($P<0.1$) response in a single trial we used a Wilcoxon rank-sum test as suggested by Hollander and Wolfe (1973), testing the null hypothesis that the ISIs in the single-trial response observation window are from the same distribution as the pooled ISIs in the spontaneous observation window. With this test we are able to detect both excitatory responses (polarity 1) and inhibitory responses (polarity -1). The polarity of the occurring rate change indicated the comparison of the mean ISI distribution. On the basis of 10 repeated presentations of each single odor we calculated the odor-specific reliability index *Ri* as the ratio of odor presentations that evoked a detectable response divided by the total number of odor repetitions [see Fig. 7]).

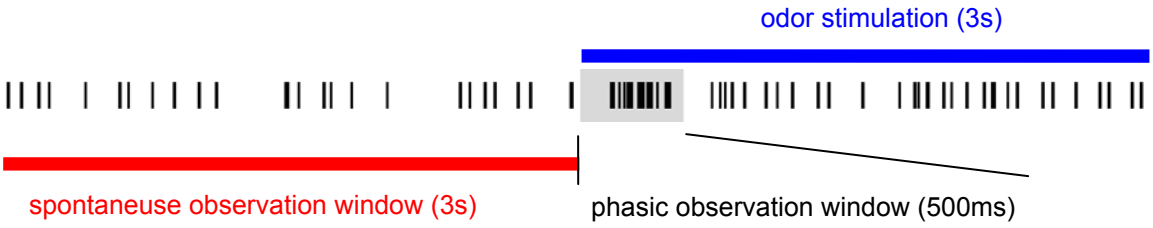

Figure 3. Response detection. *This sample spike train shows the spontaneous observation window (red) and the phasic observation window (grey). To decide if a response occurred or not, the Inter-Spike-Interval (ISI) distribution in both windows was compared. The blue bar marks the time of odor stimulation.*

Odor Specificity and Odor Tuning

Pooling ISIs across repeated presentations of the same odor in both observation windows was uses to test for a significant mean response. We quantified odor specificity for each individual neuron by the relative number of odors that evoked a significant mean response. To further quantify the odor-specific response strength in the activity of a single unit we measured the response amplitude by either (i) the trial-averaged firing rate, or (ii) the reciprocal of the mean ISI within the response observation interval. Using either measure we constructed odor tuning curves and measured the signal-to-noise ratio as described elsewhere (Mehring et al., 2003).

Visualization of the recording position

The sorting procedure allowed us to relate the different events (APs) to different units, so we then asked if it is also possible to relate the units to a special visualized neuron in the 3-D Standard Brain Atlas (Brandt et al., 2005). The Honeybee Standard Brain Atlas can be downloaded from http://www.neurobiologie.fu-berlin.de/beebrain). Two visualization methods were used. The first method was adapted from Rybak and Menzel (1993), who used Lucifer yellow (Sigma) and injected it iontophoretically into the ENs of the ventral MB. The problem we had to solve was that we were recording extracellularly with no access to the neuron's soma. Yet if during electrode insertion

tissue around our recording position were destroyed, the neurons would also absorb the dye. Therefore we dipped the tip of the electrode into Lucifer yellow before insertion. After positioning the electrode as described and running the relevant experimental procedure, the electrodes were removed and the brain was dissected and fixed in 4% formaldehyde diluted in 50% methanol for 24 hours at 4 C°. Preparations were rinsed for 20 minutes in phosphate-buffered saline (PBS; pH 6.7), diluted 1:4 in distilled water, dehydrated in an increasing ethanol series (30 %, 50 %, 70 %, 90 %, 99 %, 100 %, 10 minutes each), cleared in a mixture of 50% methyl-salicylate (MS) and 100% ethanol and embedded as whole mounts in MS in double-sided custom slides. The preparations were scanned with a confocal laser scanning microscope (Leica TCS SP2) with a Leica HC PL APO CS 10.0×0.40 UV dry lens objective. The disadvantage of using the dye at the tip of the electrode was that it was not possible to try a second time if the first insertion showed no spikes. It would have been difficult to relate the various fluorescent spots which appeared to the actual recording position. To solve this problem a second method was established in which the recording electrode, after running a successful experiment, was used as the active electrode to coagulate the tissue around the electrode's tip. The reference electrode inside the subject's eye served as the inactive electrode. Short electrical pulses of 10 volt and 10 milliseconds duration were applied with a frequency of 10 Hz for 10 minutes through the active electrode using a GRASS SD9 Stimulator (GRASS Instruments Quincy, Mass., USA). This procedure created at best a dot of auto florescence, and this only at the tip of the electrode where the neuronal activity was recorded during the experiment. After electrocoagulation the brain was dissected, fixed, rinsed, dehydrated, precleared, embedded in MS in double-sided custom slides, and scanned with a confocal laser scanning microscope as described previously.

Results

Visualization of the recording position

Two methods were used in the attempt to relate the recorded units to a special visualized neuron in the 3-D Standard Brain Atlas. Both methods emphasize that the recorded signal can actually be related to the ventral part of the alpha-lobe (Fig. 4). The electro coagulation protocol which we used was always the same (see Methods), although it led to variable findings. Figure 4 shows two examples of how the tissue reacts to the coagulation (A, B and C). In the first case after electrocoagulation a dot of auto-fluorescence became clearly visible, but it is not possible to relate this point to any single neuron (Fig. 4B). The other example shows that using the same parameters to electrocoagulate brain tissue can also result in a relatively big hole at the electrode insertion spot (Fig. 4C). It was also the ventral part of the alpha-lobe, but a more precise interpretation of the localization is not possible. The second method used Lucifer yellow at the tip of the electrode (Fig. 4D). The result is similar to that of successive electrocoagulation and a fluorescent spot appeared where the recording electrode was inserted. Thus we can say with certainty that we were recording from the ventral part of the MB´s alpha lobe; together with the depth of the electrode, which we controlled to be between 100-250 μm, we can state that the recorded ENs were possibly type A1, A2, A4, A5 or A7 (Rybak and Menzel, 1993).

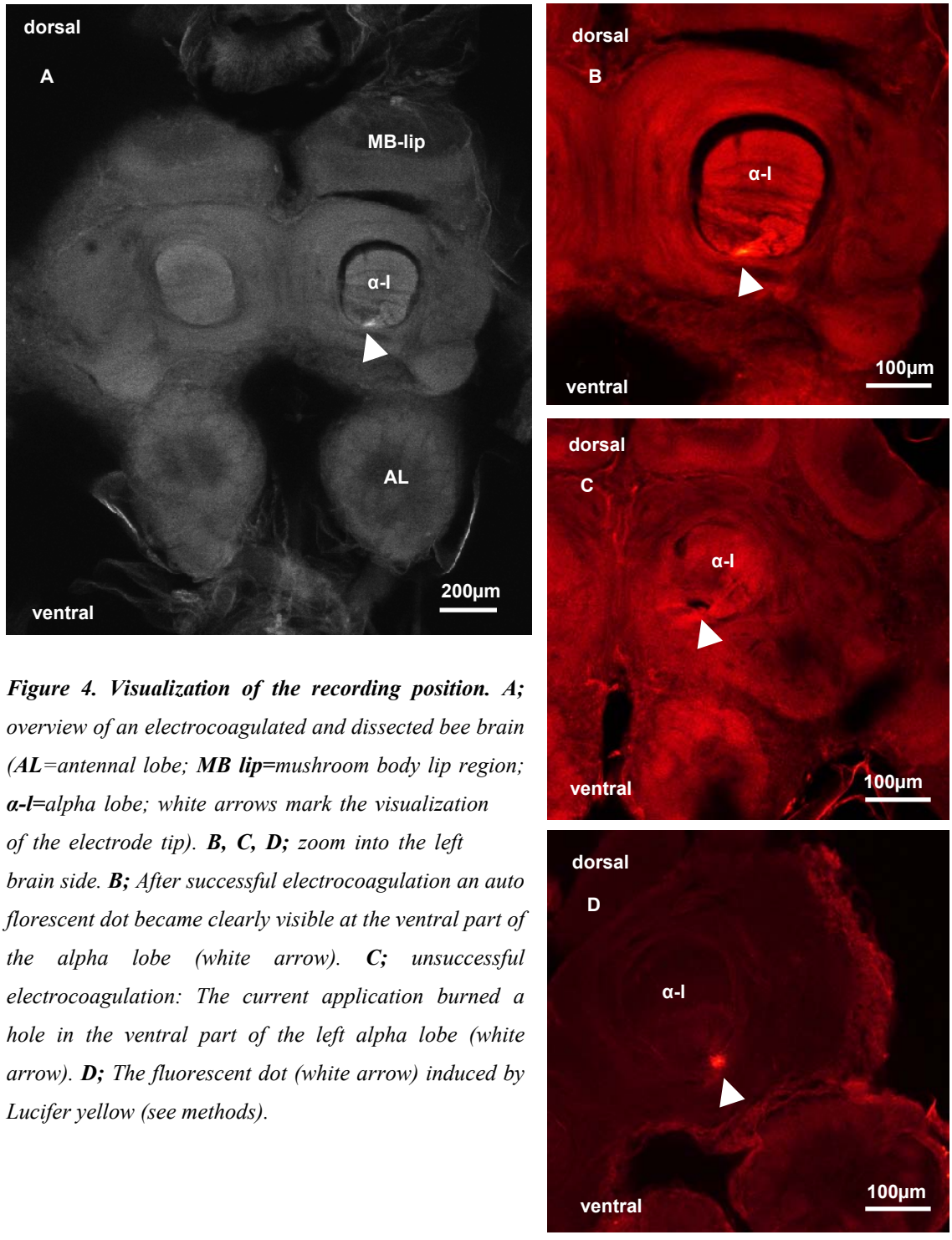

Figure 4. Visualization of the recording position. A; *overview of an electrocoagulated and dissected bee brain (**AL**=antennal lobe; **MB lip**=mushroom body lip region; **α-l**=alpha lobe; white arrows mark the visualization of the electrode tip).* ***B, C, D;*** *zoom into the left brain side.* ***B;*** *After successful electrocoagulation an auto florescent dot became clearly visible at the ventral part of the alpha lobe (white arrow).* ***C;*** *unsuccessful electrocoagulation: The current application burned a hole in the ventral part of the left alpha lobe (white arrow).* ***D;*** *The fluorescent dot (white arrow) induced by Lucifer yellow (see methods).*

Spontaneous EN activity

To characterize the spiking statistics of individual ENs we characterized their ISI distributions during the longest stationary stretch of the spontaneous activity (see Methods). First, we tested all units for a deviation from the model of a unimodal distribution (Fig. 5A). In 18 out of 51 units the ISI distribution exhibited more than one mode ($P<0.1$) indicating either a burst-like structure or possibly some non-stationary changes of the firing rate. Next, we fitted two alternative models to the empiric ISI distribution, the log-normal distribution (Fig. 5B) and the gamma distribution (Fig. 5C), and tested for significant ($P<0.05$) deviation from the respective model. We found that most neurons are best described by the log-normal model (41) and fewer by the gamma model (27). Both models are frequently used to describe the ISI distribution of regular spiking neurons.

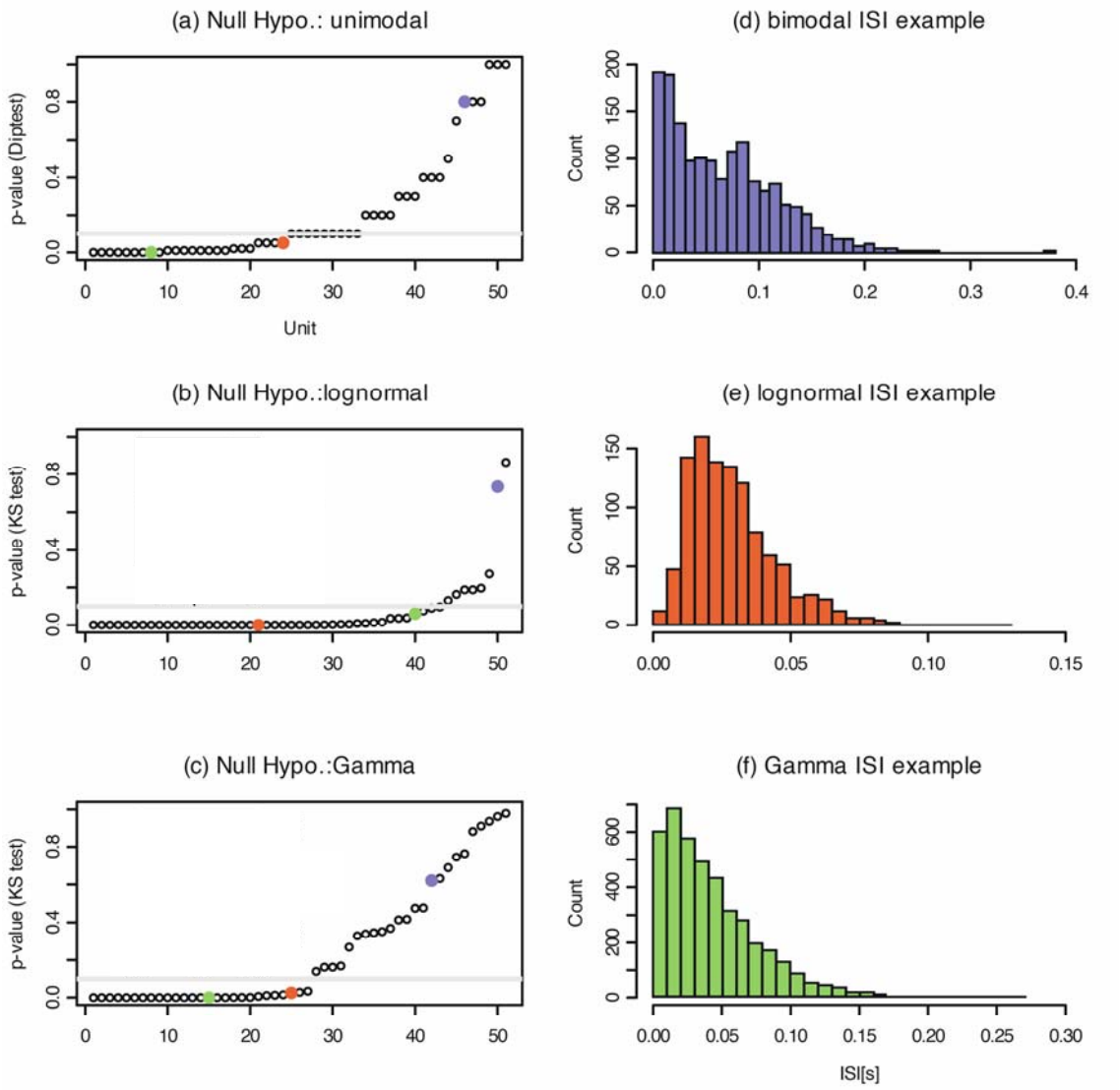

Figure 5. Inter-spike interval distributions of 51 units during spontaneous activity. *On the left; the p-values of the different units for the different statistical tests (**a**: Diptest for being not unimodal, **b:** Kolmogorov-Smirnov test for being lognormally-distributed, **c**: Kolmogorov-Smirnov test for being gamma-distributed). The grey line marked the p-value of p=0.1. On the right; the ISI distributions of three sample units (blue: bimodal ISI distribution, red: lognormal ISI distribution, green: gamma ISI distribution). The colored dots on the left are consistent with the respective sample distributions on the right.*

Initially-responding units

Units that responded to the presentation of an odor were called initial responding units. These units were characterized in the sense of their *reliability* and their odor *specificity*. To do so, 10 different odors were presented 10 times each (see Material and Methods). We observed two typical response types: excitatory responses (Fig. 6, left) and inhibitory responses (Fig. 6, right). Both could be detected by analyzing their ISI distribution before and immediately after the odor onset, as described previously (Response detection). The odor presentation lasted for 1 hour and 50 minutes in total. As the spike trains show, the recordings seemed to be very stable. The spontaneous rate of action potentials before the odor onset - and also during the air presentation - rules out cell death or loss of signal. The ongoing spontaneous firing activity during the air presentation is a valid test for contamination of the odor-supplying device with the different odors.

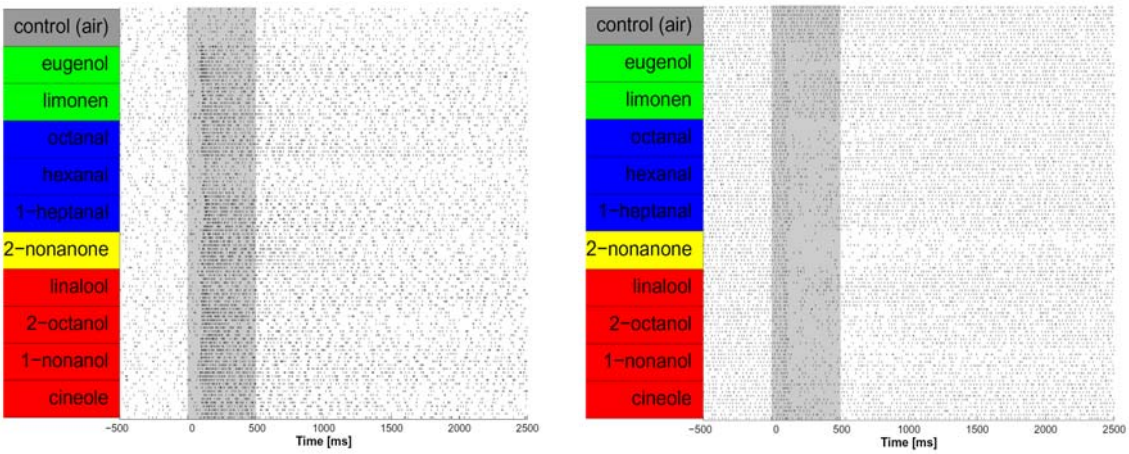

Figure 6. Two sample spike trains for 10x10 odor repetitions. *The trials are ordered for odors. Chemical groups are color-coded (Terpenes-green, aldehydes-blue, ketones-yellow, alcohols-red). The displayed units show the most dynamic changes in the first phasic part of their responses.* ***Left:*** *The odor presentation leads to an increase in the rate of the unit's spike train.* ***Right:*** *After the odor onset, the unit seems to be depressed. Light grey indicates in both cases the 500ms response detection window. Note that the stimulation lasted for a total of 3000ms. In both cases the presentation of the air (odor chamber+filterpaper+oil) seems to not facilitate a response.*

Response Reliability

One question that came up was related to the issue of reliability, because we observed that the units did not always respond to odor presentation. To quantify this we calculated the reliability index (RI; Fig. 7) for each odor. It indicates the number of trials that evoked a significant response divided by the total number of 10 repetitions. 27 single units passed through the complete experimental procedure; their RIs for the respective odor are shown in Figure 8. Most units respond to nearly all of the 10 odors, but with different RIs. Units 11, 12 and 13, for example, do not respond to most of the odors (white columns Fig. 8); presentation of only a few odors led to very unreliable responses (RI= 0,1 or 0.2 [blue columns, Fig. 8]).

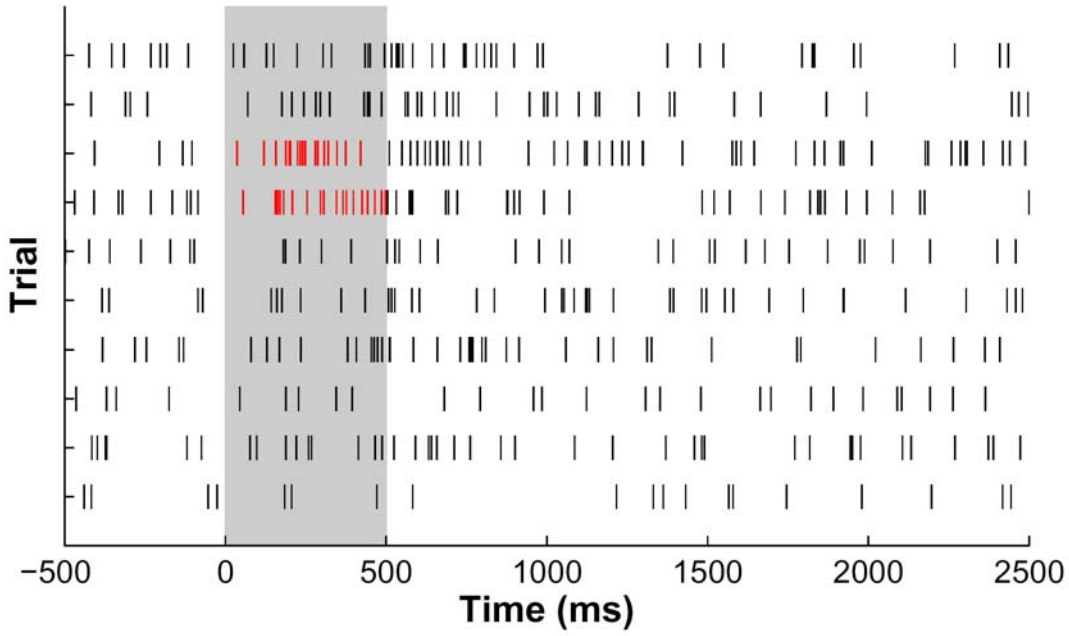

Figure 7. Dot display of an unreliable responding unit. *10 odor repetitions are shown. The odor onset was at time 0, and odor presentation lasted for 3 sec. The grey bar marked the 500 ms response detection window. Because a response is detected in only two trials (red, Wilcoxon rank-sum test significant, p<0.1) this unit has a* ***R****eliability* ***I****ndex* ***(RI)*** *of 0.2 (RI=odor presentations of one odor that evoked a response divided by the total odor repetitions)*

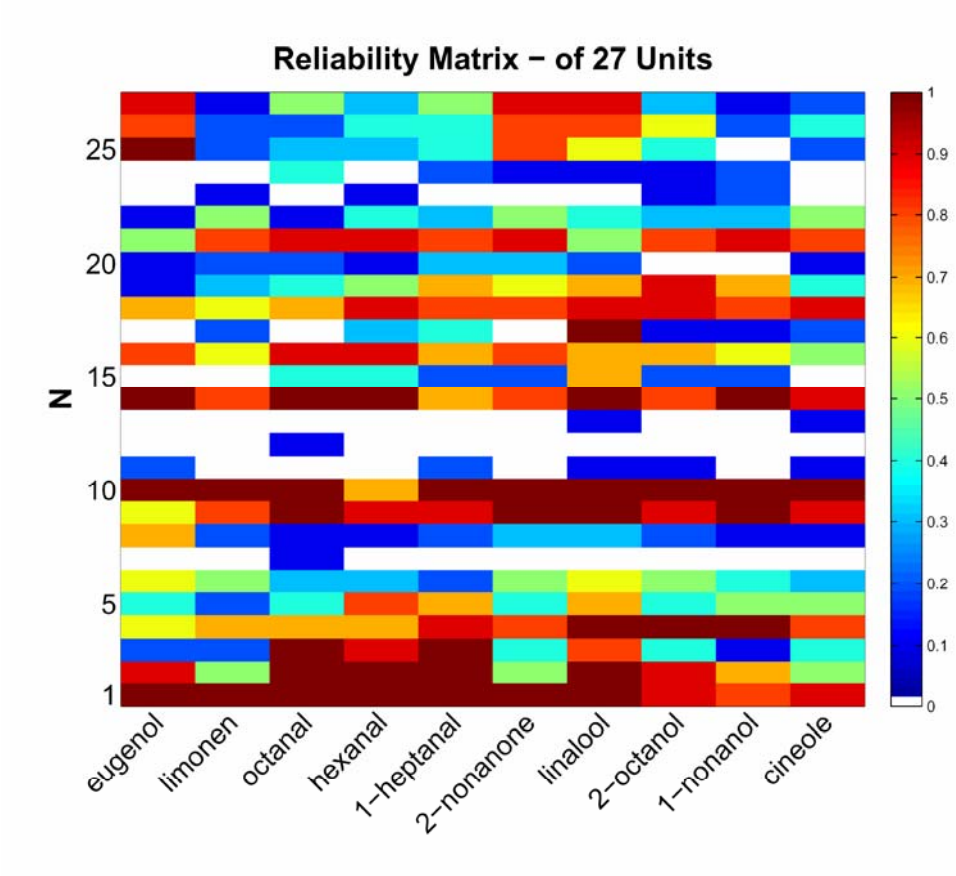

Figure 8. Reliability Matrix: *False-color coded Reliability Indices of 27 units that were stimulated with 10 trials of 10 different odors. Note that the alpha-lobe-extrinsic neurons show a broad response spectrum of reliability indices across different odors. White matrix elements refer to units that showed no response to any of the 10 repetitions of the respective odor.*

In the histogram in Figure 9 we pooled the reliability indices for all 27 units. In total there are 270 RIs (# of responding units times # of odors). From the 220 RIs (81%) which yielded a response we classified ~23% as reliable (RI>0.8; Fig. 9A, green); the other 58% are unreliable RIs. That means that the associated unit responded less than 8 times out of the 10 repetitions. Note that in ~19% of the cases not a single response was detected (RI=0; Fig. 9B, non-responding); they are related to units which are reliably non-responding to the respective odor.

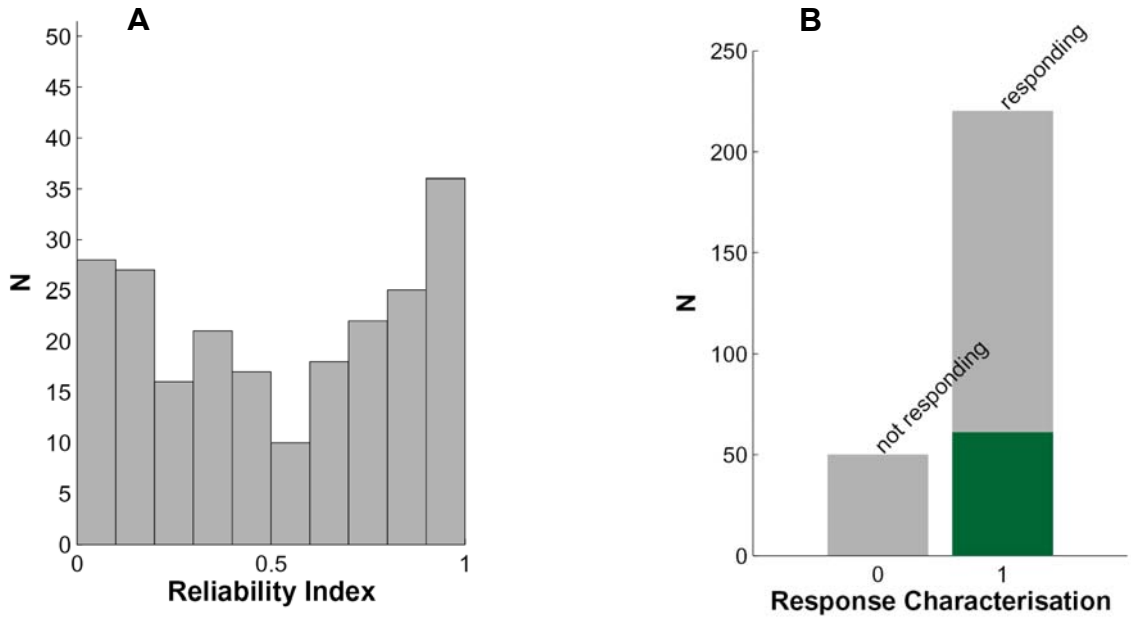

Figure 9. Reliability Index distribution (RI) of 27 units and 10 odors. *The RIs are binned and counted in 0.1 intervals.* ***A:*** *220 RIs are shown (# of responding units times # of odors). Note: only responding units are displayed.* ***B:*** *Distribution of all 270 assigned RIs. 50 reliability indices of 0 were detected (~19%). From the 220 indices which include a response ~23% are reliable (green;) the other 58% are unreliable indices. That means that the associated unit responded between 1 and 8 times during the 10 repetitions.*

Odor specificity

The next question we wanted to address was related to the issue of possible *dominant odors* that drive the units to higher reliability indices. This was not the case. For all tested odors the RIs were widely-spread (Fig. 10). For example, we found up to 7 RIs which indicated very reliable responses to linalool, 6 for limonene and lower RIs for all other odors. Note that the indices accounting for reliable not-responding units are also spread over all 10 odors (No., grey-bordered left panel in Fig. 10).

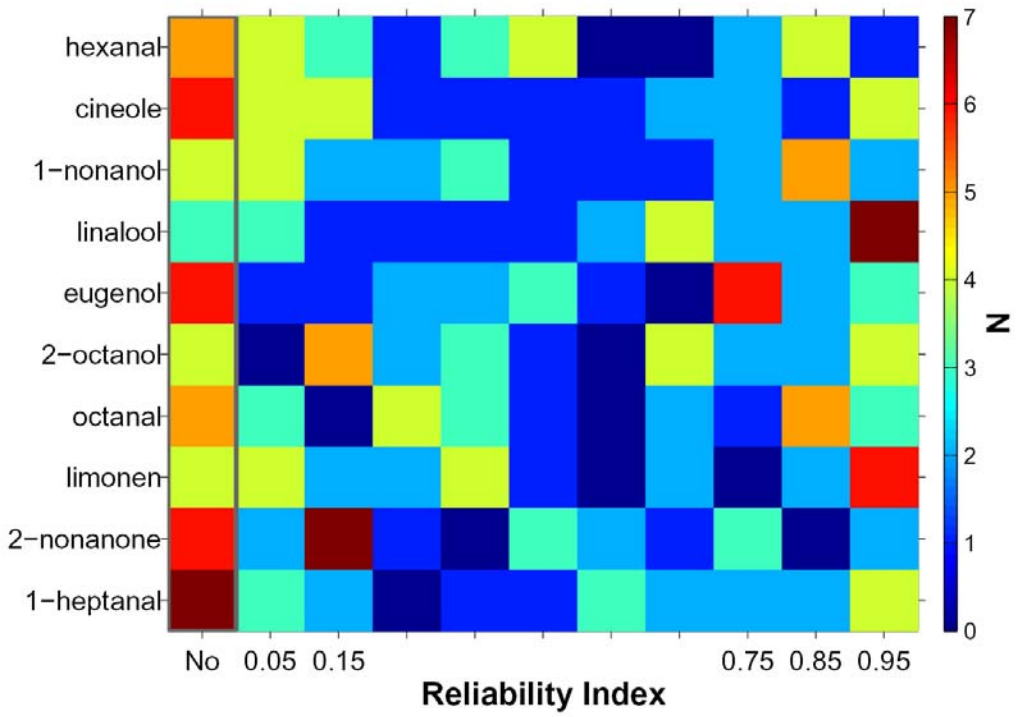

Figure 10. Odor-related Reliability Indices. *Al 270 calculated RIs (# of recorded units times # of odors) are shown in relation to the related odor. The number of assigned RIs is false-color coded (right legend). The RIs of 0 were displayed in the left, grey-framed column. Note: none of the odors could be related to more reliable responses than others.*

As the odor-related reliability indices showed, the units seem to respond to a large odor spectrum (Fig. 10). In the next paragraph we will look at the odor specificity of every single unit. Focusing on the alpha-lobe-extrinsic neurons, two types of odor responses were found: excitatory and inhibitory ones (Fig. 11). Typically, most of the presented odors lead to a response in the single unit. Figure 10 shows the average response rate for the 10 repetitions of each odor in 50 ms time bins. The false-color coded displays of the examples shown did not permit a conclusion about whether the neurons responded only to a small spectrum of odors. All stimuli facilitated an increase (Fig. 11A) or a decrease (Fig. 11B) in the firing rate of the unit. In both cases the presentation of the control air does not influence the units' spontaneous activity. Thus the odor supplying device is not contaminated with odors and the observed rate changes could be related to pure odor stimulation.

The most drastic change seems to occur in the first 500 ms after the odor onset (see Fig. 6 and Fig. 11). This phasic time window is used for calculating the tuning curves of the recorded units. We used two methods to calculate the mean response of the respective unit for the different odors (tuning curve). Both yield the same results (Fig. 12). The first method uses the pooled spike counts in the phasic time window (Fig. 12, light green). The second method uses the ISI, normalized to 1 (1/ISI; Fig. 12, dark green). For both the excitatory example unit and for the inhibitory example no clear tuning to a special odor is observable. Figure 13 showed the tuning curves of all 27 recorded units passing through the whole experimental procedure. Since the tuning curves of Figure 12 showed no difference for the two different response calculations, only the second method is used (normalized mean ISI). A clear preference of one EN to respond only to a special odor is not observable.

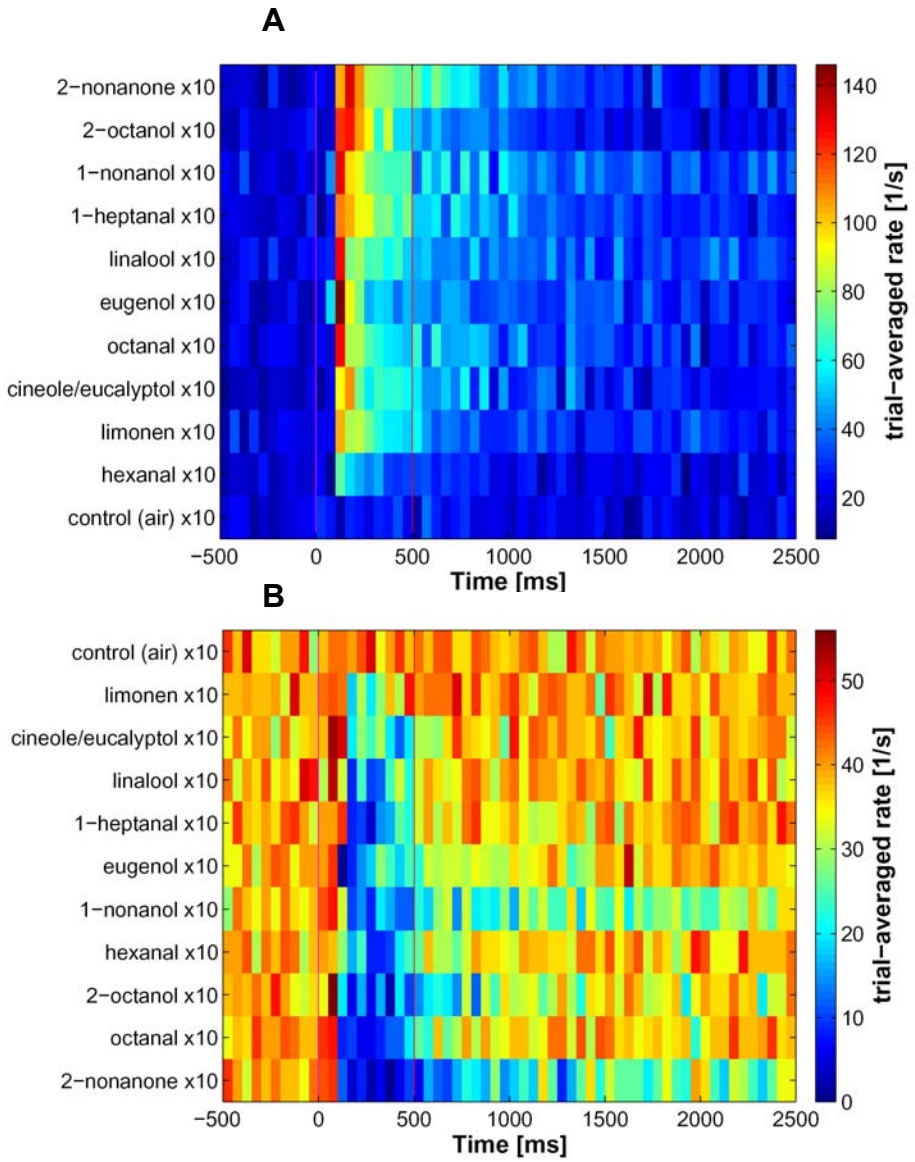

Figure 11. Trial average dynamic tuning profiles. *Two sample units (excitatory [top], inhibitory [bottom], same samples as in Figure 5). Each row represents the firing rate as a function of time measured by the PSTH (bin width 50ms) averaged across all 10 trials for one particular odor, as indicated. Firing rate is color-coded.* ***A;*** *The odors are arranged starting with the highest excitatory average rate (top) and ending with no change (air, bottom).* ***B*** *The control (air) is plotted at the top followed by the odors which evoked the weakest inhibitory response, down to 2-nonanone which led to the strongest inhibition (bottom). Stronger inhibitory responses were also prolonged in time.*

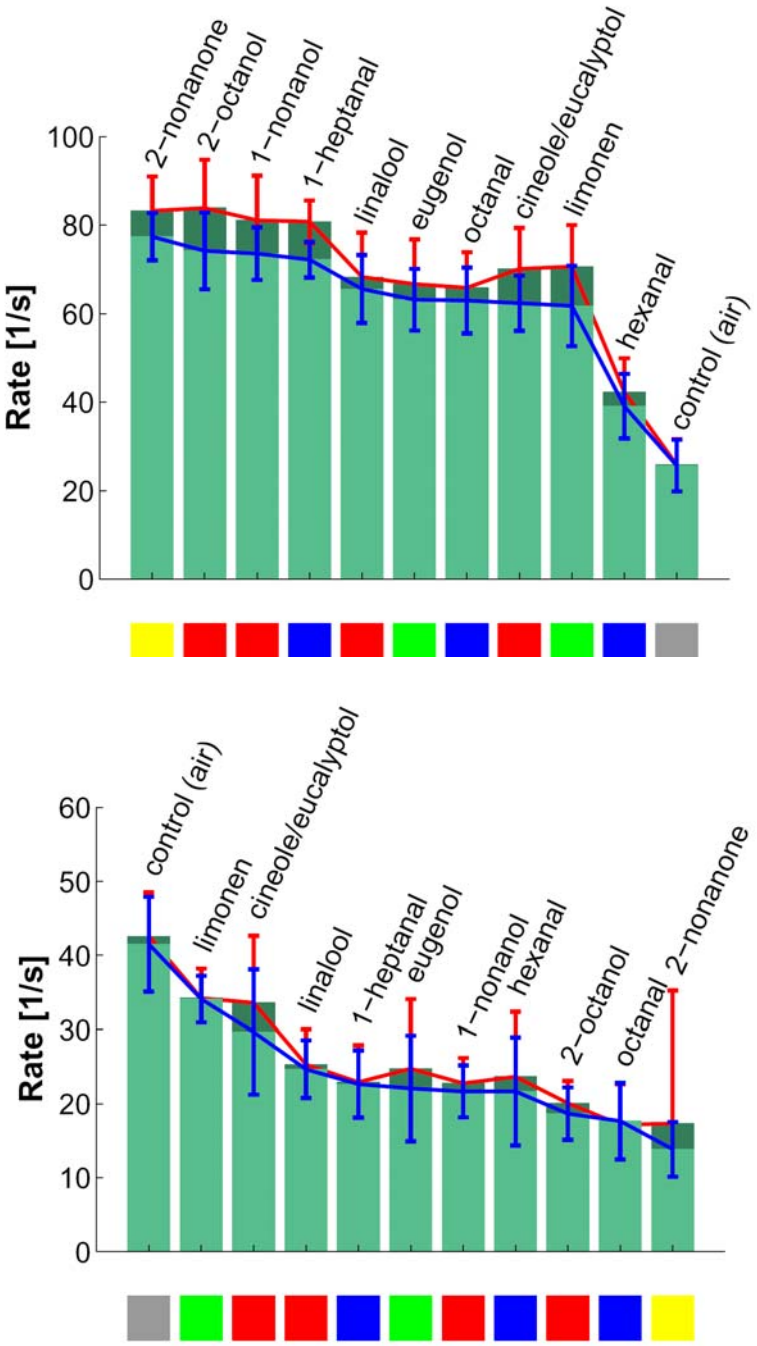

Figure 12. Odor tuning curves. *Two example units (excitatory [top], inhibitory [bottom]). Averaged firing rate as calculated in the phasic time window (500ms after odor onset) as a function of the presented odor. Two different measures are used.* ***Light green:*** *the trial-average rate is calculated from the spike count (****blue:*** *standard deviation across trials).* ***Dark green:*** *The inverse of the mean ISI within the phasic response window (****red:*** *standard deviation across intervals). Note; the spontaneous rate (baseline) is reflected by the control (air, see also Fig.11). Chemical groups are color coded (Terpenes-green, aldehydes-blue, ketones-yellow, alcohols-red).*

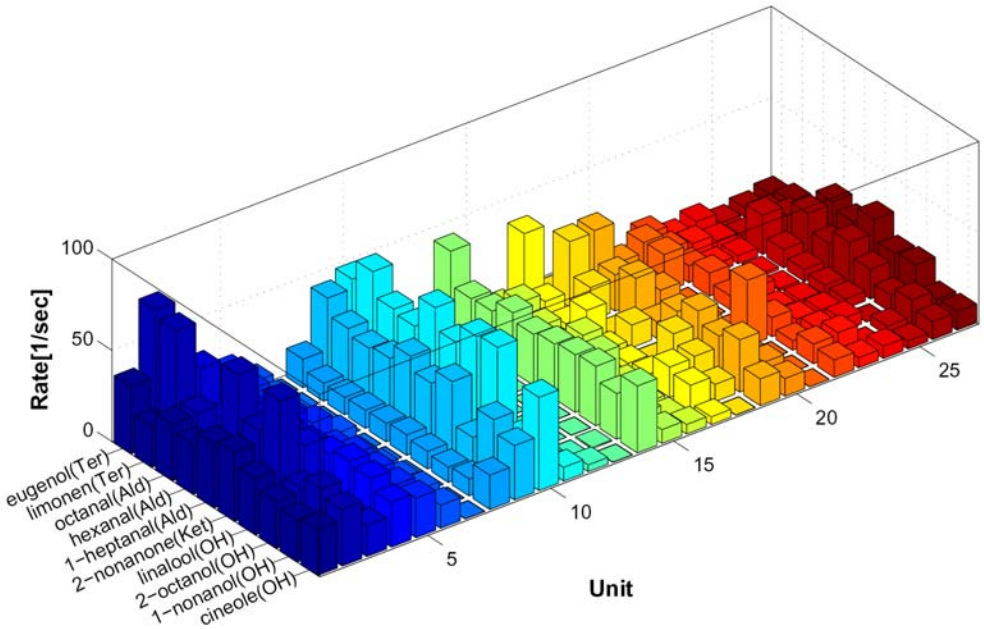

Figure 13. Tuning curves of 27 units. *All of them passed through the whole experimental procedure. The mean rates are calculated in the phasic time window (500ms after odor onset) The 1/ISI calculation was used. The baseline (spontaneous activity) was subtracted. Units 12 and 20 showed inhibitory responses (cp. Fig.1) and their polarity was flipped in this plot. For a detailed tuning curve of unit 12, see Figure 12 [bottom].*

Discussion

In the present study we extracted extracellular activity of single units which are putative mushroom body-extrinsic neurons of the honeybee. Those ENs, with their large dendrites, collect information from the high-dimensional KC activity pattern and form the output of the MB (Rybak and Menzel, 1993). Future studies will aim at learning-induced changes in the single-unit odor responses. Here we focused on solving two issues which are prerequisites for successful conduct of learning experiments. First, we had to choose an adequate recording technique. This should ensure stable observation of local single neuron behavior over many hours to be able to monitor consolidation effects after hours, or even days. Secondly, the neuronal responses to odor stimuli must be characterized in naive animals to be able to statistically compare the learning-induced changes to the naive state of the respective neuron type.

To overcome the first issue we modified the method for extracellular long-term recordings in the honeybee MB that had been successfully established by Okada et al. (2007). While they had used only two closely-spaced insulated copper wires to obtain one single differential recording combination, we added one wire and obtained 3 differential recordings. The advantage of the differential combination is that the source of the recorded signal is very close and local to the electrode tips. Interferences from other global or distant sources, such as muscle activity, were thus ruled out (Fig. 2). This is the prerequisite for a correct interpretation of a signal which is extracellularly recorded from a behaving animal. The exclusion of muscle activity from our neuronal signal is particularly important in the course of a learning paradigm where the proboscis extension response (PER) is used as a behavioral control. The PER is mediated by the M17 muscle (Rehder, 1987), the activation of which produces a strong field that is easily visible in an extracellular recording from the bee brain if the signal is not differentially recorded (cp. Fig. 2). The consequence would be a misinterpretation of the expected local neuronal change. The second advantage of this technique is that the wires we used are very thin (Ø14 µm) and flexible, so they cause only minimal damage in the brain; and by gluing the electrode to the brain surface with two-component silicon, the head capsule is simultaneously closed and the recording is stabile for up to 30 hours.

The second goal of this study was the characterization of the responses of alpha-lobe-extrinsic neurons to repeated odor stimulations. To increase the number of simultaneously-recorded ENs we adapted one additional wire to the electrode, such that we could record three differential combinations with which up to 5 different units could be recorded simultaneously (Fig. 2). Ten different odors, out of four chemical classes (see Methods), were presented, 10 times each, in an alternating sequence. After sorting the different waveforms evoked by the ENs' action potentials, we categorized the various waveforms into different units. The general response characteristics were investigated concerning their odor-specificity and the reliability of their responses to ten repetitions of one identical odor.

The activity of the recorded units can be related to alpha-lobe-extrinsic neurons

We always inserted the electrode at the ventral part of the α-lobe at a depth between 100 and 250 μm (Fig. 4.). The recorded activity in this part of the brain is dominated by ENs whose axons pass the recording field of the electrode tip and can potentially be related to the A1, A2, A4, A5 and A7 clusters. The projection fields of most EN types mentioned are restricted to only one protocerebral hemisphere, where they connect the MB with the neuropils that are located around the alpha lobe and with the lateral protocerebral lobe [LPL]; only the A7 type connects one hemisphere with the contralateral MB (Rybak and Menzel, 1993). After successful recordings we used the same electrode to electro-coagulate the tissue around the electrode tip. In some experiments the electrode tip was dipped into a fluorescent dye (Lucifer yellow). Both visualization methods were successful and the electrode position could be visualized (Fig. 4). We were not able to draw conclusions about the exact identity of the recorded ENs, but we can be certain that the electrode tip was always placed at the ventral part of the MB. Together with the differential recording combinations using the high-impedance wires (Fig. 1) we can be certain that the recorded activity is dominated by neurons located very close to the electrode tip. The recorded 27 units showed a rather variable behavior, as illustrated by the tuning curves (Fig. 13) and the broadly-distributed reliability index (Figs. 8, 9, and 10). This indicates that the recording position is not dominated by only one putative EN. Note also that inhibitory responding units could be classified.

The recorded single-unit activity can be related to non-PE1 neurons

In the case of the pedunculus-extrinsic neuron one [PE1] the extracellularly-recorded ISI distribution can be used to identify this neuron by its spike pattern (Okada et al. 2007). The PE1 shows a bimodal spiking pattern which is based on the characteristic doublets and triplets of spikes produced by this neuron which have also been described by intracellular recordings (Mauelshagen, 1993). Units confirming the bimodal distribution characteristic (Fig. 5) in our recordings cannot be related to the PE1 because it shows a characteristic peak of the higher mode at about 20-30ms. The second peak in our single-unit recordings consistently occurred at higher values (~80 ms). A second characteristic of the PE1 is its spontaneous discharge frequency of more than 15 Hz. None of our recorded units satisfied both criteria. Thus we are confident that our sample of single units did not include any PE1 neurons.

Focusing on the stationary parts of the spontaneous activity, we were able to differentiate between units that showed bimodal (18 units), and units that showed unimodal ISI distributions (Fig. 5). These differences in statistical properties might be related to different cell clusters extrinsic to the MB (cp. Rybak and Menzel, 1993). Units that displayed a unimodal distribution could be reasonably well-described by either a log-normal or a gamma interval distribution. Both distributions are prominent models for regular spiking neurons (for references see Farkhooi et al. submitted).
Another interesting question could be the learning- and consolidation-induced influence on the spontaneous rate. A unit showing lognormally-distributed ISIs before the animal had made an association, could possibly change its character to be bimodal or vice-versa. The investigation of these phenomena could shed light on the integration of a single unit into a network that computes an associated stimulus.

ENs are not involved in odor decoding

Upstream of the ENs 170,000 KCs receive second-order sensory input from different modalities innervating spatially-distinct areas of the MB calyces (Gronenberg, 1986; Mobbs, 1982; Schröter and Menzel, 2003). KCs were shown to respond highly odor-selectively and sparsely in *Drosophila* (Turner et al., 2007; Wang et al., 2004) as well as in locusts (Jortner et al., 2007; Perez-Orive et al., 2002; Stopfer et al., 2003) and in honeybees (Szyszka et al., 2005). Their axons target around 400 ENs in the vertical (α)-lobe and in the medial (β)-lobe (Kenyon, 1896; Mobbs, 1982; Rybak and Menzel, 1993). These enormous convergences from 170,000 KCs to only around 400 ENs support our view that the primary function of ENs is not to decode stimulus identitiy. Studying single ENs in different insect species has shown that these neurons are involved in learning-induced plastic changes, e.g. in the locust spike time-dependent plasticity [STDP] which occurs at the synapses between KCs and the β-lobe ENs (Cassenaer and Laurent, 2007); furthermore, in *Drosophila* a delayed memory trace is formed after 30 min only in the vertical (α-lobe) branch of the dorsal-paired medial neuron [DPM] which is an odor generalist (Yu et al., 2005). In honey bees the PE1 changed its response during classical odor conditioning (Mauelshagen, 1993). Electrical stimulation of the KC leads to the formation of associative long-term potentiation [LTP] in the PE1 (Menzel and Manz, 2005). Extracellular long-term recordings also document that the PE1 shows a reduction in the response to the rewarded stimulus after the subject has associated an odor with a reward (Okada et al., 2007). Thus there is considerable evidence that at least EN ensembles can represent a learned association that is present only after the subject has associated a conditioned stimulus [CS] with an unconditioned reward stimulus [US]. Our results support the hypothesis that ENs are not merely involved in decoding odor identity, since most of the recorded neurons respond to almost all of the ten repeated odors (Figs. 8 and 13).

EN responses are odor-unspecific

By analyzing the number of odors that evoked a response in the recorded units we found that most units show a trial-averaged response to nearly all of the 10 different odors presented. The differences in the tuning curves (Fig. 13) are likely to originate from the different pre-synaptic KC activity patterns that refer to the different odor-specific PN-bouton activities (Szyszka et al., 2005). We may hypothesize that a single EN receives input from overlapping KC activity patterns, thereby integrating different 'receptive fields'. This would explain why KC activity patterns are highly odor-specific and sparse, as has been shown in different insect species (*Drosophila*: Turner et al., 2007, Wang et al., 2004; locusts: Jortner et al., 2007, Perez-Orive et al., 2002, Stopfer et al., 2003; honey bees: Szyszka et al., 2005), while at the same time alpha-lobe-extrinsic neurons exhibit broad tuning. In the present study we used ten different odors from four chemical classes (see Methods) and presented them10 times each in an alternating sequence. The reliability indices for all individual odors averaged across different neurons (Fig. 10) do not show any preference for dominant odors or odor classes which clearly evoked more often responses than others.

EN responses are unreliable

One main result of the present study is the fact that in most single units the repeated presentation of one and the same odor stimulus resulted in a detectable response in only some of the trials, as documented by the large number of small reliability indices (Figs. 8, 9 and 10). This is the case even though the KC pattern is odor-specific and sparse across repeated trials (*Drosophila*: Turner et al., 2007, Wang et al., 2004; locusts: Jortner et al., 2007, Perez-Orive et al., 2002, Stopfer et al., 2003; honey bees: Szyszka et al., 2005). This means that some transition takes place from the level of the MB input in the KCs to the level of the MB output. What could be the mechanism that influences the transmission between the KCs and ENs?

There is a large body of evidence that the alpha-lobe-extrinsic neurons of the protocerebral calycal tract (PCT) which are GABA immunoreactive (ir) inhibitory neurons are involved in this mechanism. These neurons could be effective in two ways:

locally; by recurrently sending their collaterals down the peduncle and reaching the dendritic trees of the ENs, and by exiting the alpha lobe around its lateral midline and projecting to the input region of the mushroom body, the calyces (Okada et al., 2007). The inhibitory activity of these neurons on strategically important synapses should influence the ENs of the ventral part of the MB and possibly suppress the response to a relevant stimulus in some of the trials. Then the question is: what drives the GABA ir PCT neurons to sometimes be active and sometimes not? To work toward answering this question it is necessary to simultaneously record both types of alpha-lobe-extrinsic neurons and investigate the correlations between their respective activities. Evidence for the local impact of GABA ir PCT neurons is delivered by the alpha-lobe-extrinsic neurons that were recorded in the present study which responded very reliably with inhibition to all of the 10 presented odors (Figs. 11B, 12B and 13). This inhibition should be mediated presynaptically to the recorded unit, possibly by a PCT neuron.

In future learning experiments we will analyze whether the EN characteristics of an unspecific and unreliable response profile will be changed after the subject made an association between an odor and a reward.

Acknowledgements

We thank Ryuichi Okada for initial help in building the electrodes, and Stefan Stiller for valuable analysis of some of our data during his bachelor-degree project. We also thank Sonja Gruen and Juergen Rybak for fruitful discussions. This work was part of a cooperation hosted by the Bernstein Center for Computational Neuroscience Berlin (BCCN Berlin) and supported by grants from the Bundesministerium für Bildung und Forschung (BMBF; grant 01GQ0413).

References

Abel, R., Rybak, J. and Menzel, R. (2001). Structure and response patterns of olfactory interneurons in the honeybee, *Apis mellifera*. *J Comp Neurol* **437**,363-383.

Bicker, G., Kreissl, S. and Hofbauer, A. (1993). Monoclonal antibody labels olfactory and visual pathways in *Drosophila* and *Apis* brains. *J Comp Neurol* **335**, 413-424.

Brandt, R., Rohlfing, T., Rybak, R., Krofczik, S., Maye, A., Westerhoff, M., Hege, C. and Menzel, R. (2005). Three-dimensional average-shape atlas of the honeybeebrain and its applications. *J Comp Neurol* **492**, 1–19.

Cassenaer, S. and Laurent, G. (2007). Hebbian STDP in mushroom bodies facilitates the synchronous flow of olfactory information in locusts. *Nature* **448(7154)**, 709-713.

Dujardin, F. (1850) Memoire sur le systeme nerveux des insects. *Ann Sci Nat Zool* **14**, 195-206.

Erber, J., Masuhr, T. H., Menzel, R. (1980). Localization of short-term memory in the brain of the bee, *Apis mellifera*. *Physiol Entomol* **5**, 343-358.

Farkhooi, F., Strube-Bloss, M.F. and Nawrot, M.P. (submitted). A non-renewal point process model for neuronal spiking.

Flanagan, D. and Mercer, A. R. (1989). An atlas and 3-D reconstruction of the antennal lobes in the worker honey bee, *Apis mellifera* L. (Hymenoptera: Apidae). *Int J Insect Morphol Embryol* **18**, 145-159.

Galizia, C.G., Joerges, J., Kuttner, A., Faber, T. and Menzel, R. (1997). A semi-in-vivo preparation for optical recording of the insect brain. *J Neurosci Methods* **76**, 61-69.

Galizia, C.G., Mc Ilwrath, S.L., and Menzel, R. (1999a). A digital three-dimensional atlas of the honeybee antennal lobe based on optical sections acquired by confocal microscopy. *Cell Tissue Res* **295**, 383-394.

Gronenberg, W. (1986). Physiological and anatomical properties of optical input-fibres to the mushroom body in the bee brain. *J Insect Physiol* **32**, 695-704.

Heisenberg, M. (2003). Mushroom body memoir: from maps to models (Review). *Nat Rev Neurosci* **4**, 266-275.

Hollander, M. and Wolfe, D. (1973). Nonparametric Statistical Methods. *Wiley & Sons,* New York.

Jortner, R.J., Farivar, S.S., and Laurent, G. (2007). A simple connectivity scheme for sparse coding in an olfactory system. *J Neurosci* **27(7)**, 1659–1669.

Kenyon, F.C. (1896). The brain of the bee - A preliminary contribution to the morphology of the nervous system of the Arthropoda. *J Comp Neurol* **6**, 134-210.

Martin, J-R., Ernst, R. and Heisenberg, M. (1998). Mushroom bodies suppress locomotor activity in *Drosophila melanogaster*. *Learn & Mem* **5**, 179-191.

Mauelshagen, J. (1993). Neural correlates of olfactory learning in an identified neuron in the honey bee brain. *J Neurophysiol* **69**, 609-625.

Mehring, C., Hehl, U., Kubo, M., Diesmann, M. and Aertsen, A. (2003). Activity dynamics and propagation of synchronous spiking in locally connected random networks. *Biol Cybern* **88(5),** 395-408.

Menzel, R. and Manz, G. (2005) Neural Plasticity of Mushroom Body-Extrinsic Neurons in the Honeybee Brain. *J Exp Biol* **208**, 4317-4332.

Menzel, R., Erber, J. and Masuhr, T. H. (1974). Learning and memory in the honeybee. In: *Experimental analysis of insect behaviour* (ed. L. Barton-Browne), **pp**. 195–217. Springer, Berlin, Germany.

Milner, B. Squire, L.R. and Kandel, E.R. (1998). Cognitive neuroscience and the study of memory. *Neuron* **20**, 445-468.

Mizunami, M., Okada, R., Li, Y.S., Strausfeld, N.J. (1998). Mushroom bodies of the cockroach: Activity and identities of neurons recorded in freely moving animals. *J Comp Neurol* **402,** 501-519.

Mizunami, M., Weibrecht, J.M. and Strausfeld, N.J. (1993). A new role for the insect mushroom bodies: Place memory and motor control. In: *Biological Neural Networks in Invertebrate Neuroethology and Robotics*. (eds. R. D. Beer, R. Ritzmann, and T. McKenna) **pp.** 199–225. Academic Press, Cambridge, MA.

Mobbs, P.G. (1982). The brain of the honeybee *Apis mellifera* I. The connections and spatial organization of the mushroom bodies. *Phil Trans R Soc Lond* **B 298**, 309-354.

Müller, D., Abel, R., Brandt, R., Zockler, M. and Menzel, R. (2002). Differential parallel processing of olfactory information in the honeybee, *Apis mellifera* L. *J Comp Physiol* **188**, 359-370.

Okada, R., Ikeda, J. and Mizunami, M. (1999). Sensory responses and movement-related activities in extrinsic neurons of the cockroach mushroom bodies. *J Comp Physiol* **[A] 185**, 115-129.

Okada, R., Rybak, J., Manz, G. and Menzel, R. (2007). Learning-related plasticity in PE1 and other mushroom body-extrinsic neurons in the honeybee brain. *J Neurosci* **27(43)**:11736–11747.

Pascual, A. and Preat, T. (2001). Localization of long-term memory within the *Drosophila* mushroom body. *Science* **294,** 1115-1117.

Peele, P., Ditzen, M., Menzel, R. and Galizia, C. G. (2006). Appetitive odor learning does not change olfactory coding in a subpopulation of honeybee antennal lobe neurons. *J Comp Physiol A Neuroethol Sens Neural Behav Physiol* **192**, 1083-103.

Perez-Orive, J., Mazor, O., Turner, G.C., Cassenaer, S., Wilson, R.I., and Laurent, G. (2002). Oscillations and sparsening of odor representations in the mushroom body. *Science* **297**, 359-365.

Rehder, V. (1987). Quantification of the honeybee's proboscis reflex by electromyographic recordings. *J Insect Physiol* **33**, 501–507.

Rybak, J. and Menzel, R. (1993). Anatomy of the mushroom bodies in the honey bee brain: the neuronal connections of the alpha-lobe. *J Comp Neurol* **334**: 444-465.

Sachse, S. and Galizia, C. G. (2002). Role of inhibition for temporal and spatial odor representation in olfactory output neurons: A calcium imaging study. *J Neurophysiol* **87**, 1106–1117.

Schröter, U. and Menzel, R. (2003). A new ascending sensory tract to the calyces of the honeybee mushroom body, the subesophageal-calycal tract. *J Comp Neurol* **465**, 168-178.

Stopfer, M., Jayaraman, V. and Laurent, G. (2003). Intensity versus identity coding in an olfactory system. *Neuron* **39**, 991-1004.

Strausfeld, N. J. (1998) *review*. Crustacean-insect relationships: the use of brain characters to derive phylogeny amongst segmented invertebrates. *Brain Behav Evol* **52(4-5)**, 186-206.

Strausfeld, N. J., Hansen, L., Li, Y., Gomez, R. S. and Ito, K. (1998). Evolution, discovery, and interpretations of arthropod mushroom bodies. *Learn & Mem* **5**, 11-37.

Szyszka, P., Ditzen, M., Galkin, A., Galizia, C.G. and Menzel, R. (2005). Sparsening and temporal sharpening of olfactory representations in the honeybee mushroom bodies. *J Neurophysiol* **94**, 3303-3313.

Turner, G.C., Bazhenov, M. and Laurent, G. (2008). Olfactory representations by *Drosophila* mushroom body neurons. *J Neurophysiol* **99**, 734-746.

Wang, Y., Guo, H.-F., Pologruto, T.A., Hannan, F., Hakker, I., Svoboda, K., and Zhong, Y. (2004). Stereotyped odor-evoked activity in the mushroom body of Drosophila reavealed by green fluorescent protein-based Ca2+ imaging. *J Neurosci* **24,** 6507-6514.

Yu, D., Akalal, D.B. and Davis, R.L. (2006). *Drosophila* alpha/beta mushroom body neurons form a branch-specific, long-term cellular memory trace after spaced olfactory conditioning. *Neuron* **52**, 845-855.

Yu, D., Keene, A.C., Srivatsan, A., Waddell, S. and Davis, R.L. (2005). *Drosophila* DPM neurons form a delayed and branch-specific memory trace after olfactory classical conditioning. *Cell* **123**, 945–957.

Yu, D., Ponomarev, A. and Davis, R. L. (2004). Altered representation of the spatial code for odors after olfactory classical conditioning: memory trace formation by synaptic recruitment. *Neuron* **42**, 437–449.

Zars, T., Fischer, M., Schulz, R. and Heisenberg, M. (2000). Localization of a short-term memory in *Drosophila*. *Science* **488,** 672-675